

A Ferroresonance Case Study Involving a Series-Compensated Line in Sweden

Robert Rogersten, Robert Eriksson

Abstract—Ferroresonance is caused by the magnetic saturation of ferromagnetic materials in association with capacitive elements in power systems. In practice, such magnetic saturation often involves reactors or various types of transformers. Ferroresonance in power systems has been extensively researched in the past. However, examples of ferroresonance field measurements on series-compensated lines are scarcely represented, and therefore, ferroresonance field measurements that have been acquired on a series-compensated line in Sweden are presented within a case study. The highly distorted voltage and current waveforms resulted in an outage on a 400 kV busbar. Field measurements are compared with electromagnetic transient (EMT) simulation results within the case study. Furthermore, ferroresonance mitigation measures are proposed based on simulation results from a set of power system states with varying transformer saturation characteristics. It is shown that the states at which the power system is at high risk of ferroresonance were present during the disturbance discussed in the case study.

Keywords—Ferroresonance, series-compensated lines, power transformers

I. INTRODUCTION

FERRORESONANCE is a destructive “phenomenon” that severely impacts power quality, potentially causing damage to electrical equipment when excessive voltages and currents are induced. The word ferroresonance first appeared in the 1920s in [1] and was subsequently presented more analytically in the 1940s [2]. An even more comprehensive work was outlined in [3] in the 1950s.

Numerous examples of ferroresonance have been described in the past. Specifically, voltage transformer failures due to ferroresonance have been described in [4]. Reference [4] also discusses cases where ferroresonance occurred in autotransformers in association with the capacitive coupling of transmission lines and ferroresonance in distribution transformers with an open phase. However, examples in literature are often limited to voltage transformers with inadequate grounding or insufficient damping and distribution transformers with an open phase. Ferroresonance in power transformers is rarely demonstrated, provided that all three source phases are energized.

Ferroresonance involving series-compensated lines is a known problem since the 1930’s, significant interest arose when it was shown that the use of series capacitors for voltage regulation caused ferroresonance in distribution

systems [5]. Reference [5] emphasized that ferroresonance involving series-compensated lines is most likely to occur in association with unloaded transformers. A recent review of the literature on this topic showed that ferroresonance involving series-compensated lines has been addressed for load rejection scenarios [6]. Furthermore, a study of ferroresonance involving series-compensated lines was conducted in [7], where it was referred to as a special case that is rarely reported in the related literature. In conclusion, only a few reports on the problem of ferroresonance involving series-compensated lines exists. Additionally, previous work has mainly focused on electromagnetic transient (EMT) simulations and left out real-world field measurements. Therefore, herein, voltage and current measurements are presented within a case study to demonstrate the existence and behavior of ferroresonance from the real-world when a series-compensated line is involved.

In Sweden it has been practice to use series capacitor installations to increase the transfer capability of several high-voltage transmission lines. This study demonstrates field measurements of ferroresonant sustained waveforms on a series-compensated line. These highly distorted waveforms, showing a large content of subharmonics and harmonics, resulted in an outage on a 400 kV busbar. The nonlinear system behavior precludes an analysis performed using conventional linear circuit theory, rendering the analytic approach too complex. Time domain simulation is an efficient method to solve the complex nonlinear problem and to also develop countermeasures. The EMT simulation tool PSCAD/EMTDC is used to replicate the disturbance within the case study and to propose ferroresonance mitigation measures. The discrete Fourier transform (DFT) is used to compare the simulation results with field measurements and to analyze the subharmonic and harmonic content.

The contribution of this article is twofold. Firstly, real-world measurements are presented within an EMT simulation case study to demonstrate the existence and behavior of ferroresonance involving a series-compensated line and thereby fill this gap in the literature. Secondly, ferroresonance mitigation measures are proposed based on simulation results to henceforth avoid ferroresonance. In particular, it is shown that these mitigation measures are violated in the case study.

II. SUBHARMONIC RESONANCE

This case study presents real-world measurements that have a significant amount of the periodic subharmonic 3rd mode. Previous work [6], [7] studying ferroresonance that involves series-compensated lines also demonstrate this mode.

To arrive at a plausible understanding of the physical causes of these subharmonics consider the oscillatory electric

R. Rogersten and R. Eriksson are with the System Studies Group, Swedish National Grid, Sturegatan 1, 172 24 Sundbyberg, Sweden (e-mail: rrog@kth.se and robert.eriksson@ee.kth.se).

R. Eriksson is also with the Department of Electric Power and Energy, Royal Institute of Technology, Teknikringen 33, 100 44 Stockholm, Sweden.

Paper submitted to the International Conference on Power Systems Transients (IPST2019) in Perpignan, France June 17-20, 2019.

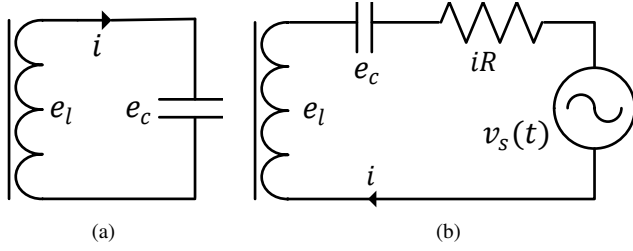


Fig. 1. Simple electric circuits subjected to magnetic saturation. In the oscillatory lossless electric circuit (a), only the natural frequency will be present. In the electric circuit (b), the frequency of the voltage source will be present in addition to the natural frequency.

Fig. 1a Wave Shapes

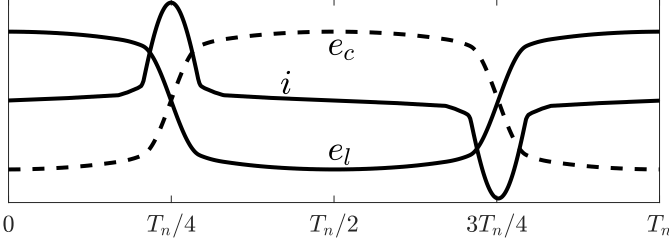


Fig. 1b Wave Shapes

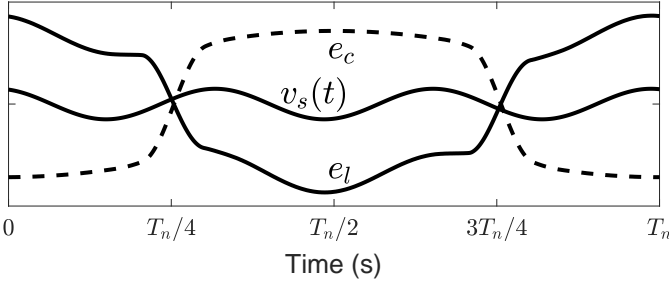


Fig. 2. Simulated wave shapes of the current and voltages saturated oscillations from the circuits shown in Fig. 1.

circuit in Fig. 1a. The actual characteristics of the oscillatory curve shapes (subject to saturation) are obtained from a PSCAD/EMTDC simulation and are shown in the upper portion of Fig. 2. Both the voltages and current are illustrated for an entire cycle of time equal to T_n . Therefore, the voltages and current angular frequency, ω_n , is given by:

$$\omega_n = \frac{2\pi}{T_n}. \quad (1)$$

In the absence of resistance, the inductive and capacitive voltages are in equilibrium with each other and oppositely equal as illustrated in the upper portion of Fig. 2. Furthermore, the current has a narrow peaked curve shape. However, the introduction of a resistance will make the amplitude of oscillations to decay. In order for the waveforms to be sustained, an external voltage source needs to counteract the losses. Therefore, consider the electric circuit in Fig. 1b, where a resistance R and a voltage source $v_s(t)$ are included. Thus, in the nonlinear oscillatory circuit, the voltage source has no other work to do than to compensate the ohmic voltage drop iR , where i is the circuit current. Therefore, resonance can be sustained if the external voltage has a value equal to iR , the smaller the resistance, the lower is the voltage necessary to sustain resonance. Consequently, the voltage source $v_s(t)$

needs to be chosen as a peaked curve shape voltage oscillation that can be expressed as a Fourier series:

$$Ri(t) = \sum_{k=0}^{\infty} b_{(2k+1)} \sin((2k+1)\omega_n t). \quad (2)$$

Quarter-wave odd symmetry has been adopted for the Fourier series supposing an ideal waveform of i as shown in Fig. 2. Therefore, only sine functions and odd coefficients are present.

Suppose the circuit in Fig. 1b is not fed by the peaked voltage expressed in (2) and instead is fed by a sinusoidal voltage source $v_s(t)$ with the angular frequency ω_f that is higher than the natural angular frequency ω_n . The ohmic voltage drop can be expressed as

$$Ri(t) = v_s(t) + \Delta e, \quad (3)$$

where Δe can be regarded as an additional residual voltage acting on the circuit. This residual voltage contains a substantial wave of the natural angular frequency ω_n , which now acts as a distorting voltage in the circuit. The current and voltages wave shapes are changed in the new circuit and therefore the natural frequency also change. Subharmonic resonance can occur if odd integer multiples of the natural angular frequency ω_n and the voltage source forced angular frequency ω_f are established. Therefore, suppose the angular frequency $3\omega_n$ (i.e., the angular frequency associated with the second term in the Fourier series in (2)) would establish at the voltage source angular frequency ω_f . Consequently, an angular frequency contained in Δe will be

$$\omega_n = \frac{\omega_f}{3}. \quad (4)$$

Thus, substantial currents and voltages correlated with $1/3$ of the supply frequency will appear on the saturated circuit. Furthermore, the higher harmonics contained in Δe will contain current and voltages correlated with angular frequencies of $5\omega_f/3$, $7\omega_f/3$, and so forth. Moreover, a certain magnitude, or magnitude between certain limits, is required by the voltage source. With greater resistance, higher voltages are necessary to balance the ohmic drop. A further increase of the circuit resistance will entirely suppress subharmonic resonance. The voltages wave shapes when 3rd mode subharmonic resonance is established are shown in the lower portion of Fig. 2.

III. CASE STUDY WITH REAL-WORLD MEASUREMENTS

The critical part of the Swedish power system is described by Fig. 3. The autotransformer station is connected to a series-compensated transmission line from a station called North and to a transmission line from a station called South. The power transfer is generally from North towards South and the active power on the series-compensated line was around 800 MW (in the transformer station) in this case study. There are two reactors installed in the transformer station. However, reactor X1 remained disconnected in the case study.

In this case study, data have been extracted from field measurements and simulations for phase a. The same study for phase b and c would be very alike that of phase a.

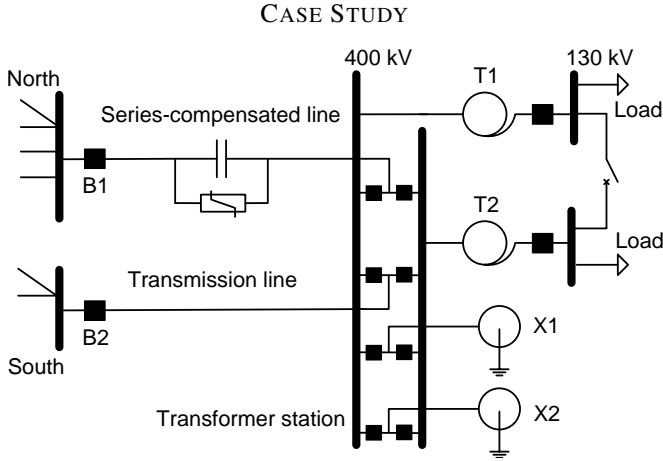


Fig. 3. Critical part of the Swedish power system used in this case study.

TABLE I
COMPONENTS RATED DATA

Object	Rated power	Rated voltage	Rated current
T1	350 MVA	400/143 kV	505 A
T2	350 MVA	400/143 kV	505 A
X1	165 MVA	420 kV	227 A
X2	165 MVA	420 kV	227 A

A. Model Implementation

With the electromagnetic transient simulation tool PSCAD/EMTDC, transformers with specified saturation characteristics, series-compensated transmission lines, and Thévenin equivalent voltage sources, can be put together to replicate the behavior of the physical components. The transmission lines from North to South are implemented using a frequency dependent model including the conductor geometry with the ground and tower components. Transmission lines connecting to North and South from adjacent stations are implemented using the Bergeron model. Furthermore, the series-compensated line between North and the transformer station is compensated to about 86%. The series compensation comprise of two capacitor banks with parallel metal-oxide varistors (MOV). Rated data for autotransformers and reactors in the transformer station are shown in Table I. The load of transformer T2 was set to correspond to 10% of the rated power during simulations. Furthermore, transformer T1 had no load in the case study.

The saturation characteristic of the autotransformer model is based on the transformer's air core reactance, the knee-point voltage, and the magnetization current. A knee-point voltage of 1.25 pu and an air core reactance of 0.3 pu have been used in the case study. The knee-point voltage is defined as the y-axis intercept with the asymptotic line of the saturation characteristics. Furthermore, the slope of that line is based on the air core reactance.

B. Field Measurements and Simulations

Three measured parameters are available for the subsystem illustrated in Fig. 3, namely, a) the phase-to-ground busbar voltage in the transformer station, b) the series-compensated line's phase current (measured in North), and c) the reactor's phase current. As discussed in [8], the use of

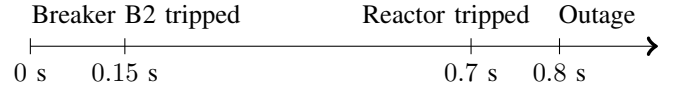


Fig. 4. Timeline that illustrates the sequence of events.

high-voltage instrument transformers for measuring power quality parameters is a complex task. The phase-to-ground busbar voltage has been measured with a capacitive voltage transformer (CVT). Therefore, accuracy is only guaranteed when the capacitive voltage divider and the electromagnetic unit are in resonance at the rated frequency, a small shift from the 50 Hz rated frequency causes errors in both amplitude and phase. However, it is still possible to make an argument using the available CVT measurement to demonstrate the presence of ferroresonance. Furthermore, the two current measurements are assumed to be reasonable accurate with regard to the current transformers and the studied frequency range. The phase-to-ground voltage in the transformer station is shown in Fig. 5, the reactor's phase current is shown in Fig. 6, and the series-compensated line's phase current is shown in Fig. 7. A timeline that illustrates the sequence of events is shown in Fig. 4. Three relevant events are associated with the timeline:

1. While testing the relay equipment in South, the relay personnel tripped the transmission line breaker B2 at about $t = 0.15$ s.
2. Owing to the large content of subharmonics, the reactor X2 tripped undesirably at about $t = 0.7$ s.
3. The transformers' differential protections tripped all 400 kV breakers at about $t = 0.8$ s.

The voltage and current waveforms are shown to be highly distorted after the breaker B2 was tripped in the first event. Furthermore, the reactor's phase current shown in Fig. 6 goes to zero in the second event. In the third event, all 400 kV breakers and the transformers' 130 kV breakers were tripped by the transformers' differential protections. Consequently, both 400 kV busbars in the transformer station were de-energized. As there are no 400 kV circuit breakers for the transformers, each transformer differential protection trips the busbar connecting the transformer to clear any transformer fault. As the transformer core was repeatedly saturated, high transformer magnetization current peaks occurred after the first event, as shown in Fig. 7. The largest current peak from field measurements exceeds 2.2 kA in North at approximately $t = 0.79$ s, i.e., shortly after the second event. The peak could be compared with the rated peak currents of both transformers $2 \cdot 505 \cdot \sqrt{2} \approx 1.43$ kA.

IV. MODEL COMPARISON AND ANALYSIS

The DFT has been used to analyze and compare EMT simulation results with field measurements. In section II, it was illustrated with a simple circuit that a subharmonic resonance frequency of 1/3 of the supply frequency can arise. Based on DFT analysis, conclusions regarding subharmonic resonance are drawn for the more complex case. A quantitative analysis of the time domain waveforms is difficult to conduct by investigating the curve shape; the key information is in the

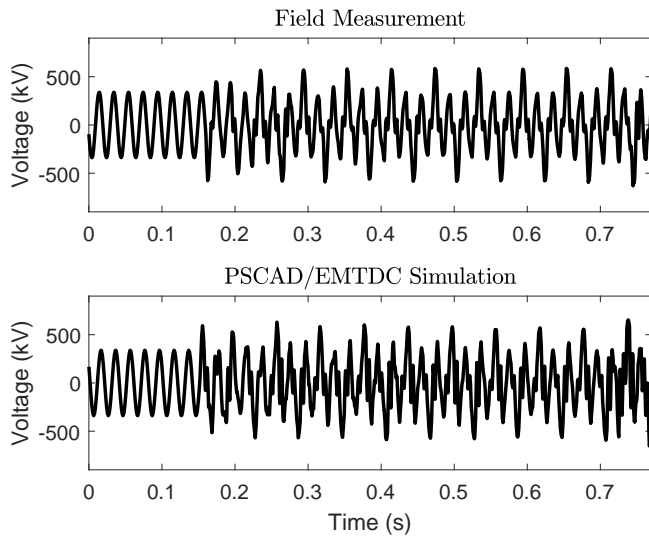


Fig. 5. Phase-to-ground voltage in the transformer station. The upper portion of the figure shows data acquired from field measurements with a sample rate of 12.8 kHz. The bottom portion of the figure shows simulation results.

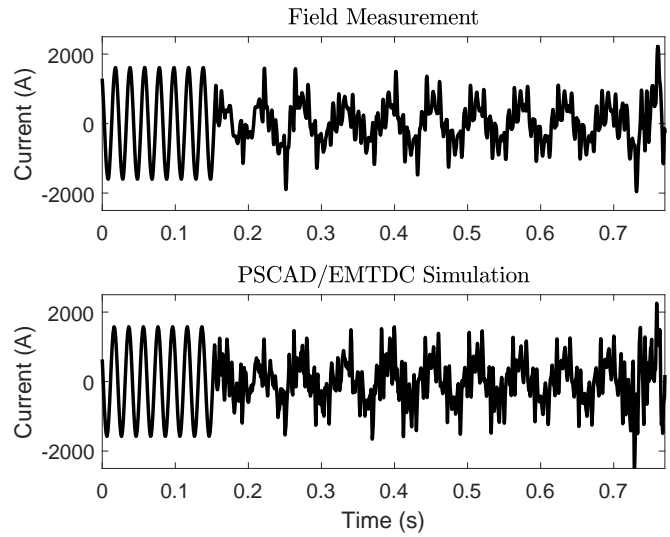


Fig. 7. The series-compensated line's phase current. The upper portion of the figure shows data acquired from field measurements in North with a sample rate of 25.6 kHz. The bottom portion of the figure shows simulation results.

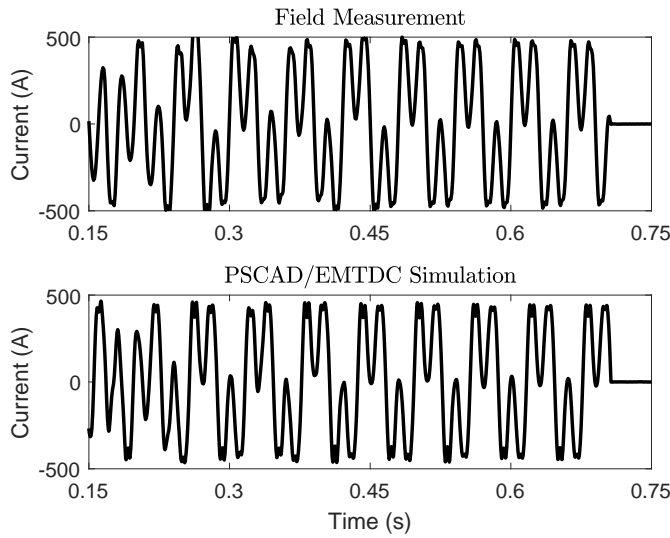


Fig. 6. The reactor's phase current. The upper portion of the figure shows data acquired from field measurements with a sample rate of 1 kHz. The bottom portion of the figure shows simulation results.

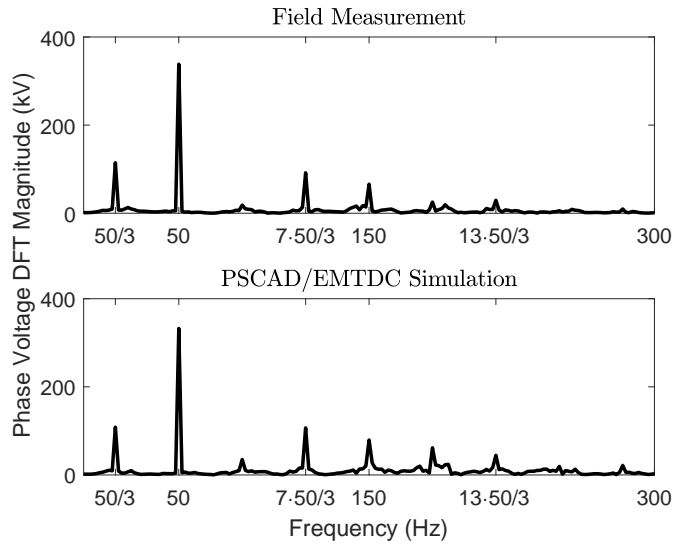


Fig. 8. The DFT magnitude of the phase-to-ground voltage in the transformer station.

frequency, phase and amplitude of the component sinusoids. The DFT is therefore used to extract the amplitude (called the DFT magnitude) of the component cosine waves.

The DFT magnitude of the phase-to-ground voltage in the transformer station is shown in Fig. 8 and is calculated from a 600 ms time window. The dominant frequency is shown to be the 50 Hz fundamental frequency. Furthermore, there is a peak at the subharmonic frequency of $50/3$ Hz ≈ 16.67 Hz and frequency peaks at odd multiples of the subharmonic frequency, where the most distinctive are $7 \cdot 50/3$ Hz ≈ 116.67 Hz and $9 \cdot 50/3$ Hz = 150 Hz. Consequently, the ninth multiple of the subharmonic can also be interpreted as the third harmonic of the 50 Hz fundamental frequency. There also exist minor peaks at $5 \cdot 50/3$ Hz, $11 \cdot 50/3$ Hz, and $13 \cdot 50/3$ Hz. The associated DFT magnitude of the reactor's phase current is shown in Fig. 9 and is calculated from a 300 ms time window. The

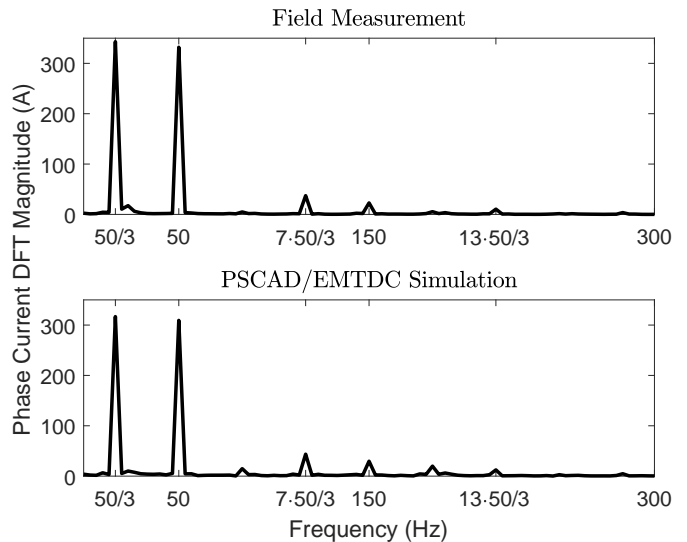


Fig. 9. The DFT magnitude of the reactor's phase current.

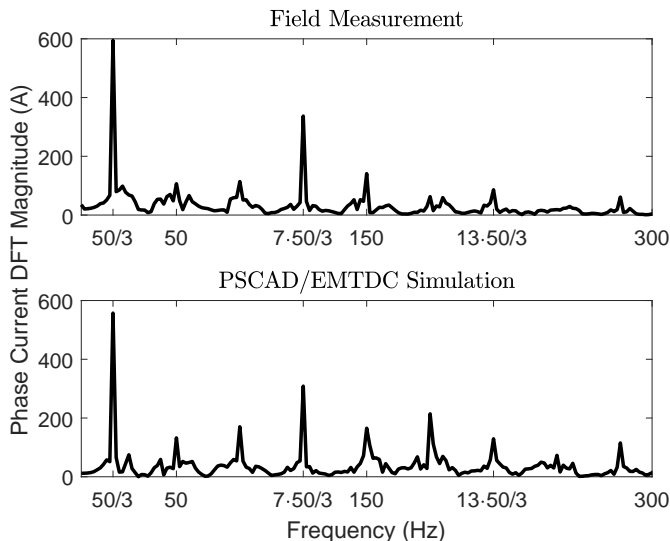


Fig. 10. The DFT magnitude of the series-compensated line's phase current.

TABLE II
TRANSFORMER SATURATION CHARACTERISTIC PARAMETERS

Set	Knee-point voltage	Air core reactance
1	1.25 pu	0.3 pu
2	1.25 pu	0.17 pu
3	1.25 pu	0.13 pu
4	1.15 pu	0.3 pu
5	1.15 pu	0.17 pu

two dominant frequencies are shown to be the subharmonic frequency of $50/3$ Hz and the fundamental frequency of 50 Hz. Furthermore, distinguishable minor peaks arise at odd multiples of the $50/3$ Hz component. Finally, the DFT magnitude of the series-compensated line's phase current is shown in Fig. 10 and is calculated from a 600 ms time window. The dominant frequency in this distorted waveform is the subharmonic frequency of $50/3$ Hz. Furthermore, frequency peaks arise at odd multiples of the $50/3$ Hz component.

Based on the DFT analysis and the time domain waveform comparison it is illustrated how the PSCAD/EMTDC model replicates the power system behavior. The resonant amplitude correlated with the frequency of $50/3$ Hz was active both during simulation and in the real-world. The magnitude of the $50/3$ Hz component is closely the same in simulations as in field measurements. Furthermore, the magnitudes of the odd multiples of this subharmonic component are very alike.

V. MITIGATION MEASURES

The risk of ferroresonant sustained waveforms was mainly evaluated based on the number of reactors connected in the transformer station and the transformers' active power. The risk is eliminated if the transmission line between the transformer station and South remains connected.

A. Reactors Influence on the Case Study

As previously discussed, only one reactor was connected in the case study. Therefore, the first event associated with the timeline shown in Fig. 4 was repeated but with both reactors connected. The simulated current and voltage waveforms are shown in Fig. 11. Most of the subharmonic content would have been already attenuated before the second event on the

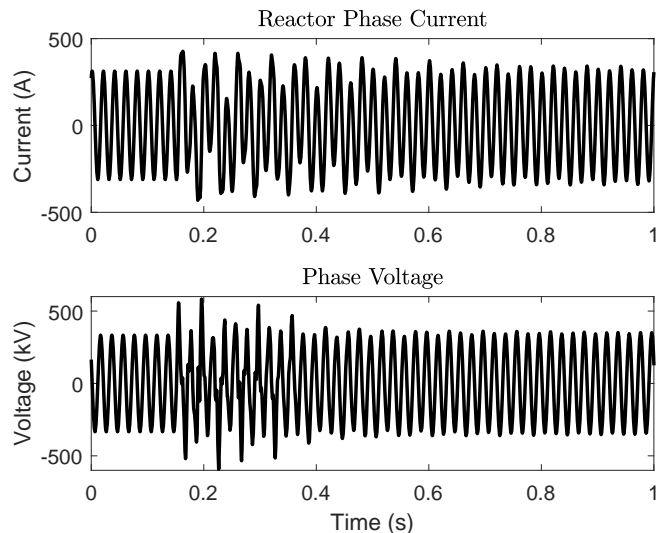


Fig. 11. The reactor's phase current and the phase-to-ground busbar voltage in the transformer station.

timeline and most likely there would have been no sustained ferroresonant waveforms when the line breaker B2 (shown in Fig. 3) in South was tripped. Hence, the risk of ferroresonance will decrease with the number of reactors connected.

B. Ferroresonance Risk Diagram

The transformers' saturation characteristic is unknown. Therefore, to establish the sensitivity of ferroresonance to the saturation characteristic, 5 sets of saturation data were used according to Table II. A ferroresonance risk diagram is shown in Fig. 13, where each set of parameters refer to the data shown in Table II. The ferroresonance risk diagram was constructed based on simulations where a three-phase fault was applied on the line between the transformer station and South, after 100 ms the fault was cleared by disconnecting the line. These simulations were conducted with all sets of saturation characteristic data and with a varying number of reactors connected in the transformer station. A lower limit for the transformers' active power was first determined when one reactor remained disconnected. To determine the limit, the active power was increased in 10% steps. As illustrated in Fig. 12, the ferroresonant waveforms are attenuated if the active power is at 30% the rated value or above. Furthermore, the procedure was repeated with both reactors disconnected, where lower limits of 40% and 50% were determined. At last, simulations were conducted with both reactors connected where no ferroresonant sustained waveforms could be induced. The pre-fault active power transfer from North towards the transformer station was 800 MW in each case.

To test the risk of ferroresonance when the transmission line remains connected, a three-phase fault was applied at one of the 130 kV busbars in the transformer station. The fault was cleared together with the load. Simulations were conducted with the transformers' active power set to 10% and the pre-fault active power transfer set first to 800 MW, and second to 510 MW, resulting in different post-fault active power transfers. Simulations were also conducted with the transformers' active power set to 50% using the same pre-fault active power transfers. The distorted voltage waveforms

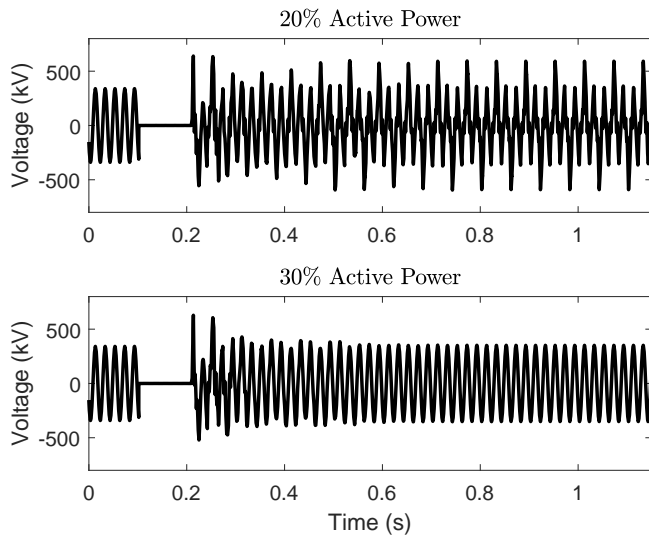


Fig. 12. Voltage waveforms in the transformer station. A three-phase fault was applied on the line between the transformer station and South at $t = 0.1$ s. The fault was cleared after 100 ms by disconnecting the line.

were attenuated after the fault with all sets of saturation characteristic data and with both reactors disconnected. Thus, the risk of ferroresonant sustained waveforms is eliminated if the transmission line remains connected.

C. Risk Diagram Correlation With the Case Study

Based on actual power system's state estimations, the load curve of transformer T1 during the year of the disturbance is shown in Fig. 14. A moving average filter has been used to smoothen out the curve; therefore, the transformer's active power could be different between certain power system state estimations. An observation from Fig. 14 is that the ferroresonant sustained waveforms were observed in October when the active power was practically zero. Moreover, the power of transformer T2 was also low during that time. Consequently, after the line was tripped in the first event on the timeline shown in Fig. 4, the power system was in the "high risk" zone shown in Fig. 13.

D. Risk Diagram Limitations

To readily interpret when the ferroresonance risk is high, the diagram in Fig. 13 was constructed with some limitations. The diagram was constructed under the assumption that the transformers' active power is equally distributed. Furthermore, it was assumed that no meshed connections or active generating units existed in the 130 kV grids. However, this is in general not true. Furthermore, the transformers' reactive power was assumed to be zero. This is approximately correct for the smoothen moving average curve of the reactive power shown in Fig. 14. However, in reality the reactive power will not always be zero. The type and timing of the fault also affect the outcome of Fig. 13.

VI. CONCLUSIONS

In this case study, ferroresonance field measurements have been presented to demonstrate the real-world existence and behavior when a series-compensated line is involved. Furthermore, the DFT has been used to compare simulation

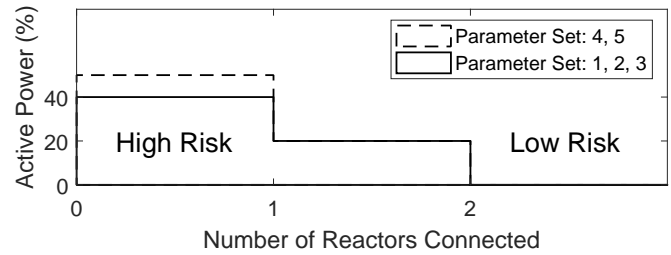


Fig. 13. Ferroresonance risk diagram evaluated based on the transformers' active power and the numbers of reactors connected in the transformer station.

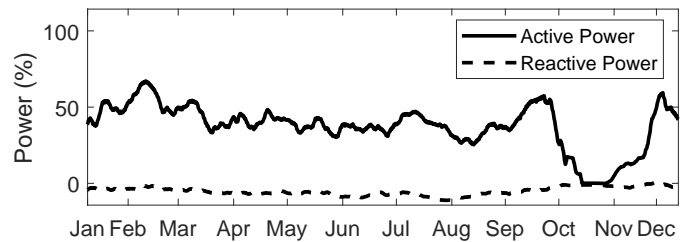


Fig. 14. The load curve of transformer T1 during the year of the disturbance. The load curve is obtained from a power system state estimator.

results with field measurements. Specifically, it was shown from field measurements and simulations that a significant amount of the periodic subharmonic 3rd mode appeared during ferroresonance. Additionally, mitigation measures have been determined based on transmission line faults. The correlated finding shows that there is a risk of ferroresonance when the transformers' active power is low. Moreover, the risk of ferroresonance decreases if the number of reactors connected in the transformer station increases. These operational conditions were shown to be violated in the case study. To ensure secure operation multiple solutions are possible, e.g., an awareness of the power system state, or an automatism to bypass the series capacitor when the transmission line is tripped.

REFERENCES

- [1] P. Boucherot, "Existence de deux régimes en ferrorésonance," *R.G.E.*, pp. 827–828, Dec 1920.
- [2] R. Rüdenberg, *Transient performance of electric power systems*. New York, NY: McGraw-Hill Book Company, 1950, ch. 48.
- [3] C. Hayashi, *Nonlinear Oscillations in Physical Systems*, ser. McGraw-Hill electrical and electronic engineering series. McGraw-Hill, 1964.
- [4] M. R. Iravani, A. K. S. Chaudhary, W. J. Giesbrecht, I. E. Hassan, A. J. F. Keri, K. C. Lee, J. A. Martinez, A. S. Morched, B. A. Mork, M. Parniani, A. Sharshar, D. Shirmohammadi, R. A. Walling, and D. A. Woodford, "Modeling and analysis guidelines for slow transients - Part III: The study of ferroresonance," *IEEE Transactions on Power Delivery*, vol. 15, no. 1, pp. 255–265, Jan 2000.
- [5] J. W. Butler and C. Concordia, "Analysis of series capacitor application problems," *Transactions of the American Institute of Electrical Engineers*, vol. 56, no. 8, pp. 975–988, Aug 1937.
- [6] W. Chandrasena and D. A. N. Jacobson, "Application of a protection scheme to mitigate the impact of load rejection in a 500 kv transmission system," in *2011 IEEE Electrical Power and Energy Conference*, Oct 2011, pp. 140–145.
- [7] K. Gauthier and M. Alawie, "A special case of ferroresonance involving a series compensated line," in *International Conference on Power Systems Transients*, 2017.
- [8] "Instrument transformers – the use of instrument transformers for power quality measurement," International Organization for Standardization, Geneva, CH, Standard, May 2012.